



Identification of sodium channel toxins from marine cone snails of the subgenera *Textilia* and *Afonsoconus*

Kirsten L. McMahon¹ · Henrik O'Brien² · Christina I. Schroeder^{1,3} · Jennifer R. Deuis¹ · Dhananjeyan Venkatachalam¹ · Di Huang¹ · Brad R. Green² · Pradip K. Bandyopadhyay² · Qing Li^{4,5} · Mark Yandell⁴ · Helena Safavi-Hemami² · Baldomero M. Olivera² · Irina Vetter¹ · Samuel D. Robinson^{1,2}

Received: 9 July 2023 / Revised: 20 August 2023 / Accepted: 22 August 2023 / Published online: 9 September 2023
© The Author(s) 2023

Abstract

Voltage-gated sodium (Na_v) channels are transmembrane proteins that play a critical role in electrical signaling in the nervous system and other excitable tissues. μ -Conotoxins are peptide toxins from the venoms of marine cone snails (genus *Conus*) that block Na_v channels with nanomolar potency. Most species of the subgenera *Textilia* and *Afonsoconus* are difficult to acquire; therefore, their venoms have yet to be comprehensively interrogated for μ -conotoxins. The goal of this study was to find new μ -conotoxins from species of the subgenera *Textilia* and *Afonsoconus* and investigate their selectivity at human Na_v channels. Using RNA-seq of the venom gland of *Conus (Textilia) bullatus*, we identified 12 μ -conotoxin (or μ -conotoxin-like) sequences. Based on these sequences we designed primers which we used to identify additional μ -conotoxin sequences from DNA extracted from historical specimens of species from *Textilia* and *Afonsoconus*. We synthesized six of these μ -conotoxins and tested their activity on human $\text{Na}_v1.1$ – $\text{Na}_v1.8$. Five of the six synthetic peptides were potent blockers of human Na_v channels. Of these, two peptides (BuIIIB and BuIIIE) were potent blockers of $\text{hNa}_v1.3$. Three of the peptides (BuIIIB, BuIIIE and AdIIIA) had submicromolar activity at $\text{hNa}_v1.7$. This study serves as an example of the identification of new peptide toxins from historical DNA and provides new insights into structure–activity relationships of μ -conotoxins with activity at $\text{hNa}_v1.3$ and $\text{hNa}_v1.7$.

Keywords Conotoxin · μ -conotoxin · Voltage-gated sodium channel · Historical DNA

Introduction

Voltage-gated sodium (Na_v) channels are transmembrane proteins responsible for the initiation and propagation of action potentials in excitable cells. In humans, there are nine Na_v channel subtypes ($\text{Na}_v1.1$ – $\text{Na}_v1.9$) with distinct expression profiles and functions [1]. $\text{Na}_v1.1$, 1.2, 1.3 and 1.6 are predominately expressed in the central nervous system, $\text{Na}_v1.7$, 1.8 and 1.9 in the peripheral nervous system, and $\text{Na}_v1.4$ and $\text{Na}_v1.5$ in skeletal muscle and cardiac tissue, respectively. Na_v channel dysfunction is associated with numerous neurological disorders, including epilepsy and chronic pain [2] and compounds that selectively modulate individual subtypes are important tools to study the function of Na_v channels and have the potential to serve as drug leads.

Numerous and diverse classes of toxins have evolved to target and modulate Na_v channels [3–5]. μ -Conotoxins are peptides from the venoms of marine snails of the genus

Kirsten L. McMahon and Henrik O'Brien contributed equally.

✉ Samuel D. Robinson
sam.robinson@uq.edu.au

¹ Institute for Molecular Bioscience, The University of Queensland, St Lucia, QLD 4072, Australia

² Biology Department, University of Utah, Salt Lake City, UT 84112, USA

³ Peptide Therapeutics, Genentech, 1 DNA Way, South San Francisco, CA 94080, USA

⁴ Department of Human Genetics, Utah Center for Genetic Discovery, University of Utah, Salt Lake City, UT 84112, USA

⁵ Cancer Bioinformatics, Huntsman Cancer Institute, University of Utah, Salt Lake City, UT 84112, USA

Conus [6], which bind to “site 1” of Na_v channels, where they block Na⁺ conductance by occluding the channel pore [7]. They comprise 18–26 amino acid residues with six cysteine residues arranged in a CC–C–C–CC pattern and are derived from the “M gene superfamily” of conotoxins [8, 9].

The first μ-conotoxin described was GIIIA (along with several homologous peptides) from the venom of *Conus (Gastridium) geographus* Linnaeus, 1758 [6]. GIIIA blocked rat skeletal muscle Na⁺ current, with no discernible effect on that of nerve or brain, providing some of the earliest evidence of the existence of distinct Na_v subtypes and demonstrating the capacity of μ-conotoxins to selectively block these subtypes [6]. Since then, a number of other μ-conotoxins have been described from the venoms of other *Conus* species [10]. While the majority of these, like GIIIA, have a preference for the skeletal muscle Na_v channel (Na_v1.4) over other subtypes, several “neuronal subtype-preferring” μ-conotoxins have also been described. For example, KIIIA from the venom of *Conus (Afonsoconus) kinoshitai* Kuroda, 1956 [11] was most potent at the neuronal subtype Na_v1.2 over Na_v1.4 and was also active at Na_v1.7 (rat channels). Several efforts have been made to improve the selectivity and investigate the analgesic activity of KIIIA [12–15], and it has served as a useful tool in determining the three-dimensional structure of Na_v1.2 [16]. BuIIIB from the venom of *Conus (Textilia) bullatus* Linnaeus, 1758 [17] was a potent blocker of rNa_v1.3 [18]. As with KIIIA, efforts have been made to tune the selectivity of this peptide for Na_v1.3 over Na_v1.4 [19, 20].

μ-Conotoxins have so far been restricted to the venoms of fish-hunting and closely related lineages of *Conus*, and of these, the subgenera *Afonsoconus* and *Textilia* appear to be a promising source of “neuronal subtype-preferring” μ-conotoxins. However, for species from these subgenera other than *C. (T.) bullatus*, it is difficult to acquire live specimens for venom analysis. For example, *Conus (Textilia) dusaveli* (H. Adams, 1872) was, for more than a decade, known by a single shell found by a fisherman in the stomach of a fish caught at 60 fathoms (110 m) off Mauritius [21]. *Conus (Afonsoconus) bruuni* Powell, 1958 was formally described only in 1958, after its discovery from deep-water dredging by the Galathea expedition off the remote Pacific Kermadec islands [22].

In this study, we generated a venom gland transcriptome of *C. (T.) bullatus*, from which we identified several new μ-conotoxin sequences. We used these, and previously reported sequences, to design “μ-conotoxin-specific” primers which we used to amplify additional new μ-conotoxin sequences from DNA extracted from historical specimens of *C. (T.) dusaveli*, *Conus (Textilia) adamsonii* Broderip, 1836 and *C. (A.) bruuni*. We then synthesized several of the identified μ-conotoxins and profiled their activity at human Na_v channel subtypes Na_v1.1 to Na_v1.8.

Methods

Specimens

C. (T.) bullatus was collected from Caw-oy, Olango, the Philippines. A foot tissue sample of *C. (T.) adamsonii* was acquired from the AAMP Malacology collection of the Muséum National D'histoire Naturelle, Paris. The sample was from a specimen (IM-2013-40001) collected at a depth of 6–12 m near Ua-Pou, Marquesas Islands, French Polynesia as part of the Pakaihi I Te Moana expedition, 2012. A foot tissue sample of *C. (A.) bruuni* was acquired from the Samadi, Lozouet and Castelin malacology collection of Muséum National d'Histoire Naturelle, Paris. The sample was from a specimen (IM-2009-18222) collected at a depth of 300–320 m in the Antigonía seamount, Norfolk Ridge, New Caledonia as part of the Terrasses expedition, 2008. A single specimen of *C. (T.) dusaveli* was sourced April 2006 from Balut Island, the Philippines. The whole body had initially been stored in 70% ethanol and was noticeably degraded before being transferred to 95% ethanol and stored at 4 °C.

For species names we have followed the classification proposed by Puillandre et al. [23].

Venom gland transcriptome of *C. (T.) bullatus*

The whole venom gland of one adult specimen of *C. (T.) bullatus* was removed, immediately placed in RNALater and stored at –80 °C. Total RNA was isolated from the homogenized venom gland using TRIzol reagent following the manufacturer’s protocol (Life Technologies Corporation). Integrity of RNA was verified on a Bioanalyzer instrument (Agilent Technologies), and Illumina libraries were prepared by Cofactor Genomics. An indexed library was constructed with a mean insert size of 170 bp with the Illumina TruSeq mRNA Sample Prep Kit with oligo(dT) selection. 101 cycle paired-end sequencing was performed on an Illumina HiSeq2000 instrument (in a batch of six indexed samples). Adapter trimming of de-multiplexed raw reads was performed using fqtrim [24], followed by quality trimming and filtering using prinseq-lite [25]. Error correction was performed using the BBnorm ecc tool, part of the BBtools package. Trimmed and error-corrected reads were assembled using Trinity (version 2.2.1) [26] with k-mer length of 31 and minimum k-mer coverage of 10. Assembled transcripts were annotated using a blastx [27] search (*E* value setting of 1e–3) against a combined database derived from UniProt and Conoserver [28]. TPM counts were generated using the Trinity RSEM [29] plugin (align_and_estimate_abundance) and

expression data analysed using the trinity utilities: abundance_estimates_to_matrix and contig_ExN50_statistic. Conotoxin-encoding transcripts were extracted, trimmed to open-reading frame and redundant, partial and/or poorly expressed transcripts (< 1 TPM) discarded. The fidelity of each assembled conotoxin transcript was then manually checked using the Map-to-Reference tool of Geneious, version 8.1.7 [30]. Erroneous transcripts were discarded, while unassembled variants were manually rebuilt and added back to the final data set. Relative TPM counts were generated using the Trinity RSEM plugin (align_and_estimate_abundance) and expression data analysed using the trinity utility abundance_estimates_to_matrix.

DNA extraction

DNA was extracted from the foot tissue of *C. (T.) adamsonii*, *C. (A.) bruuni*, *C. (T.) bullatus* and *C. (T.) dusaveli* using the e.Z.N.A. Mollusc DNA Kit (OMEGA bio-tek), according to the manufacturer's instructions. Quality and yield of extracted DNA was examined by gel electrophoresis and using an Epoch Microplate Spectrophotometer (BioTek). Extracted DNA was stored at -20°C .

PCR, cloning and sequencing

Primers for amplifying μ -conotoxins were designed based on conserved regions in the propeptide and 3' UTR of *C. (T.) bullatus* μ -conotoxins, KIIIA (*C. (A.) kinoshitai*) and SIIIA (*C. (T.) striatus*). Primary PCR was performed using Advantage 2 DNA Polymerase (Clontech), sense primer 5' TGCAGAGCGTATGCAGGA 3' and antisense primer 5' TCTGAGCAAGACTGCAATCAT 3'. Nested PCR was performed using Advantage 2 DNA Polymerase sense primer 5' TGCAGGACGACATTTTCATCT 3' and antisense primer 5' GACATTGATGTAGCCGTGATA 3'. Nested PCR products were diluted, ligated into pGEM-T Easy vector (Promega), and cloned in *E. coli* DH10B competent cells (Novagen). Bacteria containing the insert from nested PCR were grown overnight in LB with ampicillin. Plasmids were isolated using the Qiaprep Spin Miniprep Kit (Qiagen) and sequenced using T7 and SP6 primers at the University of Utah Sequencing Core Facility.

Peptide synthesis

Synthetic BuIIIB, BuIIID, BuIIIE, AdIIIA, DIIIA and BIIIA were assembled by solid-phase peptide synthesis on a Liberty Prime automatic synthesizer (CEM), on rink amide-AM resin (0.1 mmol/g) using 9-fluorenylmethoxycarbonyl (Fmoc) methodology. Peptides were cleaved from solid support and side chains simultaneously deprotected in 92.5% TFA (trifluoroacetic acid)/2.5% triisopropylsilane/2.5%

$\text{H}_2\text{O}/2.5\%$ 3,6-dioxa-1,8-octanedithiol for 2 h at room temperature. Excess TFA was evaporated by N_2 flow, followed by peptide precipitation in ice-cold diethyl ether and centrifugation. Peptides were redissolved in 50% acetonitrile and lyophilized prior to oxidation.

DIIIA was thermodynamically oxidized in 0.1 M ammonium bicarbonate pH 7.5, 100 \times GSH and 10 \times GSSG for 2 h with stirring. BuIIIB, BuIIID, BuIIIE, AdIIIA, and BIIIA were synthesized with protecting groups trityl (Trt), acetamidomethyl (Acm) and 4,4'-dimethylsulfinylbenzhydryl (Msbh) with connectivity CysI–CysIV (Msbh)/CysII–CysV (Acm)/CysIII–CysVI (Trt) for regioselective oxidation. The peptides (2 mg/mL) were dissolved in acetic acid and stirred at room temperature. Five equivalents of free Trp were added to minimize side-reactions with iodine. I_2 solution (20 mg/mL) was added dropwise until the reaction turned pale-yellow and the color persisted. Following 15 min of stirring, the reaction was diluted with H_2O and hydrochloric acid to a final concentration of 50% acetic acid (v/v) and 1% hydrochloric acid (v/v). Next, eight equivalents of I_2 were added to the reaction and stirred for a further 30 min. The reaction was quenched with aqueous ascorbic acid (10 mM) until the solution became colorless. The intermediate product was isolated by reversed phase-high-performance liquid chromatography (RP-HPLC) and fractions containing the desired product were identified by electrospray ionization–mass spectrometry (ESI–MS), pooled and lyophilized. To remove the Msbh protecting groups and form the final disulfide bond, peptides were dissolved in TFA (1 mg/mL) and cooled on ice. Five equivalents of free Trp, dimethyl sulfate (1% v/v) and 20 equivalents of NaI were added and stirred for 15 min. The reaction was quenched by diluting with aqueous ascorbic acid (10 mM; 15 \times the initial volume of TFA). The final product was isolated by RP-HPLC using a Phenomenex, 5 μm C18 110 Å, 250 \times 5 mm column and a linear gradient 5–25% over 40 min. Fractions containing the desired product confirmed by ESI–MS were pooled, lyophilized and stored at -20°C . Analytical RP-HPLC and ESI–MS were used to confirm the purity and mass, respectively, of each of the folded products.

BIIIA was also synthesized as above with the alternative cysteine framework CysI–CysV (Msbh), CysII–CysIV (Acm), CysIII–CysVI (Trt). This synthetic isomer is referred to as BIIIA-iso2.

Whole-cell patch-clamp electrophysiology

Activity was assessed in Human Embryonic Kidney (HEK) 293 cells stably expressing the α -subunit of human $\text{Na}_v1.1$ – $\text{Na}_v1.7$ plus the $\beta1$ subunit (SB Drug Discovery) and Chinese Hamster Ovary (CHO) cells stably expressing human $\text{Na}_v1.8$ plus the $\beta3$ subunit in a tetracycline-inducible system (ChanTest). Cells were maintained on Mimium

Essential Medium Eagle supplemented with 10% Foetal Bovine Serum, 2 mM L-glutamine, and selection antibiotics as previously described [31], in an incubator at 37 °C with 5% CO₂ and passaged every 3–4 days (at 70–80% confluency) using TrypLE Express (Thermo Fisher Scientific).

Whole-cell patch-clamp experiments were performed using a QPatch16 II automated electrophysiology platform (Sophion Bioscience, Ballerup, Denmark) using single-hole (QPlate 16 with a standard resistance of 2 ± 0.4 MΩ) or multi-hole (QPlate 16X with a standard resistance 0.2 ± 0.04 MΩ, Na_v1.8 only). Whole-cell currents were filtered at 8 kHz and acquired at 25 kHz and the linear leak was corrected by P/4 subtraction.

The extracellular solution (ECS) contained 145 mM NaCl (replaced with 70 mM choline chloride, 70 mM NaCl for Na_v1.4, Na_v1.5 and Na_v1.7), 4 mM KCl, 2 mM CaCl₂, 1 mM MgCl₂, 10 mM HEPES, and 10 mM glucose (pH 7.4; osmolarity 305 mOsm). The intracellular solution (ICS) contained 140 mM CsF, 1/5 mM EGTA/CsOH, 10 mM HEPES, and 10 mM NaCl (pH 7.3; osmolarity 320 mOsm). TTX (1 μM) was added to the ECS for Na_v1.8 recordings to inhibit background endogenous TTX-sensitive current in CHO cells. Peptides were diluted in ECS with 0.1% Bovine Serum Albumin (BSA). Concentration–response experiments were performed using a holding potential of –90 mV and a 50-ms pulse to –20 mV (+ 10 mV for Na_v1.8) every 20 s (0.05 Hz), after a 5-min incubation of each concentration of peptide. Concentration–response curves were generated by normalizing peak current to buffer control and fitted to a four-parameter Hill equation with variable Hill coefficient: $y = \text{Bottom} + (\text{Top} - \text{Bottom}) / (1 + 10^{(\text{LogIC}_{50} - x) \times \text{HillSlope}})$.

Statistics

Data were plotted and analysed using Prism v9.0.0 (GraphPad Software). Statistical significance was defined as $P < 0.05$. All data are presented as mean ± SEM. Selectivity profiles are based on differences in potency determined by

ordinary one-way ANOVA with Tukey’s multiple comparisons test.

Data availability

The nucleotide sequences of Bu3.4 (BuIIID), Bu3.8 (BuIIE), Bu3.5, Bu3.6, Bu3.7, Bu3.9, Bu3.10, Bu3.11, Bu3.12, D3.1, Ad3.1 (including its intronic sequence) and B3.1 have been deposited at DDBJ/EMBL/GenBank [Accessions: OR128446–OR128457]. Sequences of all additional conotoxins identified in the venom gland transcriptome of *C. (T.) bullatus* are provided as Supplementary file 2.

Results

Diverse μ-conotoxin-encoding transcripts are expressed in the venom gland of *C. (T.) bullatus*

Using RNA-seq we generated a transcriptome of the venom gland of *C. (T.) bullatus* and used it to search for transcripts encoding M-superfamily conotoxins. We identified a total of 12 putative M-superfamily μ-conotoxin-encoding sequences (Fig. 1), including the previously described BuIIIA, BuIIIB, BuIIIC [17] and an orthologue of Bu17 (23/26 sequence identity) [32]. Other conotoxins identified in the venom gland transcriptome are listed in Supplementary file 2. Each of the 12 putative M-superfamily μ-conotoxin-encoding sequences encoded putative mature peptides that shared the typical sequence features of other μ-conotoxins, i.e., the CC–C–C–CC pattern (framework III), a four residue N-terminal ‘tail’ (predicted on the basis of the dibasic propeptide cleavage sites (KR) of each precursor), amidated C-termini (predicted on the basis of the C-terminal amidating enzyme recognition motif motif (G or GRR) of each precursor) and three and five residues in their intercysteine loops 2 and 3, respectively. A conspicuous feature was the diversity in the length of intercysteine loop 1, which ranged from four residues in BuIIIA to 17 residues in Bu3.11 and Bu3.12.



Fig. 1 Diverse μ-conotoxin-encoding transcripts are expressed in the venom gland of *C. (T.) bullatus*. Signal peptides and predicted mature peptides are underlined in purple and blue, respectively. Cysteine residues of the mature peptides are highlighted yellow

Extraction of DNA and sequencing of μ -conotoxin sequences from museum specimens

We used a sequence alignment of previously reported μ -conotoxin transcripts, including those of *C. (T.) bullatus*, to design multiple sets of μ -conotoxin gene-specific primers (see “Methods” section). Forward and reverse primers were designed to complement the propeptide and 3'-UTR regions, respectively, bounding the predicted μ -conotoxin mature peptide region (Fig. 2a).

We extracted DNA from ~30 mg of foot tissue from historical specimens of *C. (A.) bruuni* and *C. (T.) adamsonii* (provided by the Muséum National d'Histoire Naturelle, Paris, collected in 2008 and 2012, respectively, and stored at room temperature in 95% ethanol) and *C. (T.) dusaveli* (collected in 2006 and stored at room temperature in 70% ethanol). *C. (T.) bullatus* venom gland tissue (stored in RNAlater at -80°C for ~1 y) was used as a positive control. DNA extracted from each ethanol-stored foot tissue produced a smear across the complete molecular weight range when examined by gel electrophoresis, while that from the venom gland of *C. (T.) bullatus* produced a single sharp high molecular weight band (Fig. 2b).

The first round of PCR (30 cycles) for each extracted DNA sample, yielded multiple products ranging from 1 to 4 kb (Fig. 2c). We performed a second round of “nested” PCR (30 cycles), which yielded major products of ~3.5 kb for each sample.

Nested PCR products (~3.5 kb) were ligated into pGEM-T Easy vector for Sanger sequencing. Sequencing of the ligated vector was performed using T7 and SP6 primers to sequence from each end of each ~3.5 kb PCR product. Using this approach, we were able to sequence for each PCR product, one stretch that contained part of exon 2 (which included part of the propeptide, and for two of the three conotoxins, the *N*-terminus of the mature peptide) and a complementary stretch which contained part of exon 3, including the remainder of each mature peptide as well as some of the 3' UTR. With additional iterative primer design sequencing we sequenced the complete intervening intron of the sequence from *C. (T.) adamsonii* (Ad3.1) confirming a length of 3477 bases (Supplementary Fig. S1), consistent with the size of the nested PCR product (~3.5 kb). We analysed each sequence for exon/intron and intron/exon boundaries and “stitched” the exons together to yield the short stretch of contiguous open-reading frame encoding each μ -conotoxin mature peptide. The sequences were translated and *N*- and *C*-terminal peptide maturation sites predicted on the basis of alignments with previously described μ -conotoxin sequences, yielding the putative μ -conotoxin mature peptide sequences. For each species (*C. (A.) bruuni*, *C. (T.) adamsonii* and *C. (T.) dusaveli*), a

single putative μ -conotoxin sequence was amplified: D3.1 (DIIIA) from *C. (T.) dusaveli*, Ad3.1 (AdIIIA) from *C. (T.) adamsonii* and B3.1 (BIIIA) from *C. (A.) bruuni* (Fig. 2e).

The mature peptide sequence of each of the three new putative μ -conotoxins had a type III cysteine framework (CC–C–C–CC). DIIIA and AdIIIA each had an *N*-terminal extension of three residues, while BIIIA lacked the *N*-terminal extension (i.e., two to four residues preceding the first cysteine) seen in all other μ -conotoxins. On the basis of the presence of an amidating enzyme recognition motif (GR or GRRR) at the *C*-terminus of all three sequences, each were predicted to exist in the respective venoms with a *C*-terminal amidation. A comparison of the mature peptide sequences of each of the new putative μ -conotoxins from *C. (T.) bullatus*, *C. (A.) bruuni*, *C. (T.) adamsonii* and *C. (T.) dusaveli* to previously reported μ -conotoxins is shown in Fig. 3. DIIIA is very similar to CIIIA from the venom of *Conus (Pionoconus) catus* Hwass in Bruguière, 1792, sharing 18 of 22 aligned residues, with the only major difference occurring at the *N*-terminus. AdIIIA shares 100% identity in inter-cysteine loops 2 and 3 (nine residues) with SmIIIA from *Conus (Pionoconus) stercusmuscarum* Linnaeus, 1758, while its loop 1 sequence resembles that of BuIIIC from *C. (T.) bullatus*. BIIIA shows no obvious similarity to other μ -conotoxins, including KIIIA/B from the venom of consubgeneric *C. (A.) kinoshitai*.

Synthesis and regioselective folding of μ -conotoxins

We selected six of the peptides (BuIIIB, BuIIID, BuIIIE, AdIIIA, DIIIA and BIIIA) for testing at Na_v channels and prepared these using solid phase peptide synthesis. We initially attempted undirected thermodynamic folding of AdIIIA, DIIIA and BIIIA; however, using this strategy, of the three peptides only DIIIA folded into a single well-defined major product.

With three disulfides, μ -conotoxins can theoretically fold into 15 possible cysteine connectivities. Where examined, native μ -conotoxins have a cysteine connectivity of CysI–CysIV, CysII–CysV, CysIII–CysVI [34, 35], as do active synthetic μ -conotoxins [36, 37] (although synthetic KIIIA, under certain in vitro folding conditions favours, and is also active, with a CysI–CysV, CysII–CysIV, CysIII–CysVI connectivity) [38]. Thus, we prepared AdIIA, BIIIA, BuIIIB, BuIIID and BuIIIE using a regioselective approach, whereby each Cys in the disulfide pair, CysI–CysIV, CysII–CysV, CysIII–CysVI, were protected with Msbh, Acn or Trt, respectively. This enabled formation of disulfides in a stepwise fashion resulting in folded peptides with the canonical disulfide connectivity.

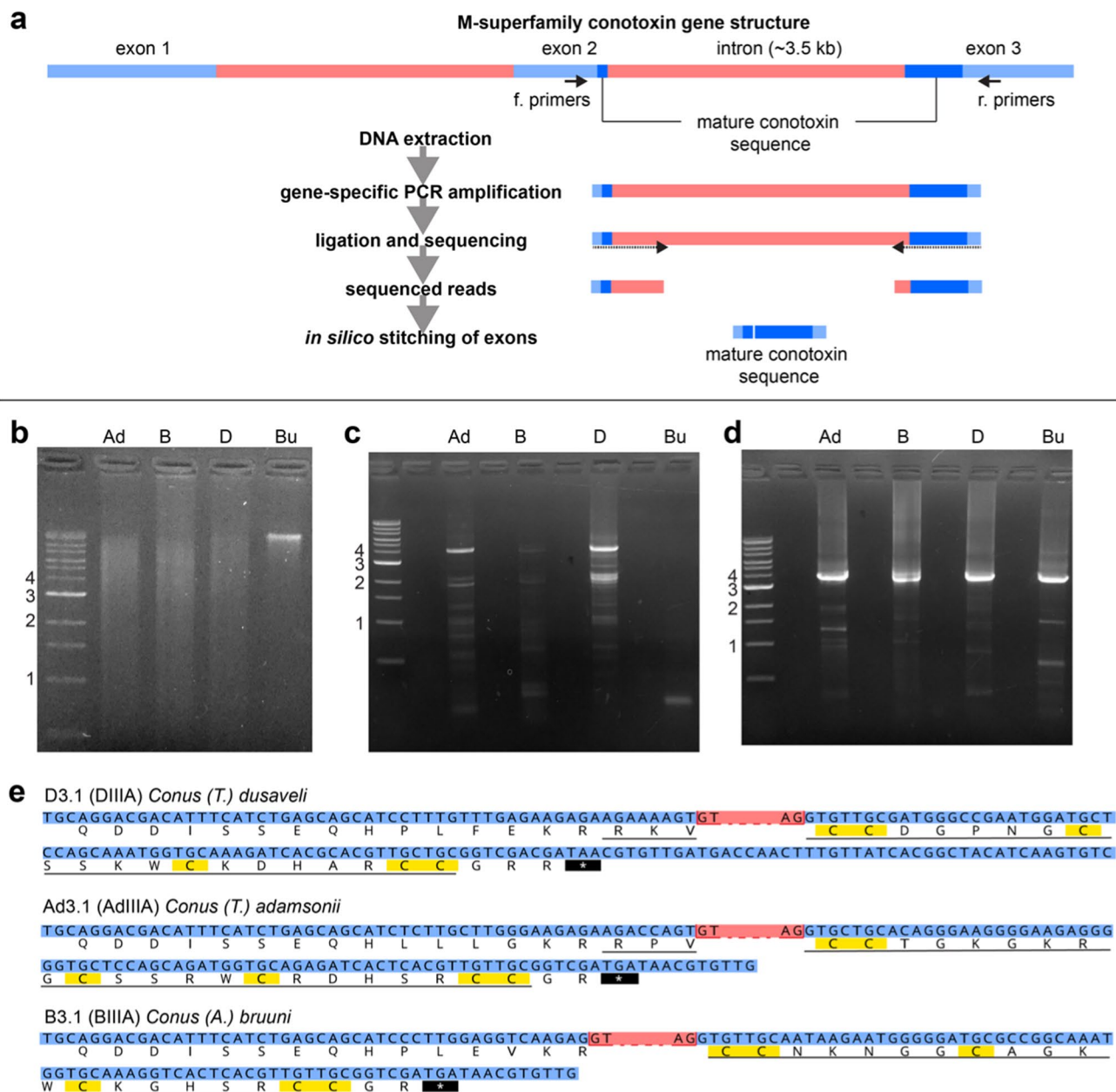


Fig. 2 DNA extraction, targeted amplification and sequencing of μ -conotoxins. **a** Experimental design: the complete precursor sequences of M-superfamily conotoxins span 3 exons, divided by two introns [33]. The mature conotoxin sequence is split between exons 2 and 3. Primers were designed targeting exon 2 and exon 3 to amplify sequences encoding μ -conotoxin mature peptides from extracted DNA. PCR products were ligated into a vector, transformed and sequenced. Complementary sequenced reads were stitched in silico to give the complete putative μ -conotoxin mature peptide sequence. **b** Gel electrophoresis of DNA extracted from *Conus* tissue samples. From left to right: *C. (T.) adamsonii*, *C. (A.) bruuni*, *C. (T.) dusaveli*, *C. (T.) bullatus* (100 μ g of DNA loaded for each). All DNA, except from *C. (T.) bullatus*, was extracted from foot tissue that had been stored in 95% ethanol at room temperature for 5–11 y. *C. (T.) bul-*

latus DNA was extracted from a venom gland stored in RNAlater at -80°C for ~ 1 y. **c** Gel electrophoresis of first round PCR products. From left to right: *C. (T.) adamsonii*, *C. (A.) bruuni*, *C. (T.) dusaveli*, *C. (T.) bullatus*. **d** Gel electrophoresis of nested PCR products, each showing a strong band at ~ 3.5 kb. From left to right: *C. (T.) adamsonii*, *C. (A.) bruuni*, *C. (T.) dusaveli*, *C. (T.) bullatus*. **e** μ -conotoxin sequences detected from *C. (T.) adamsonii*, *C. (A.) bruuni* and *C. (T.) dusaveli*. Exon nucleotide sequence are colored blue, while intervening intron nucleotide sequence are colored red. Intron sequence has been removed for clarity showing only the first two nucleotides at each boundary. Translated sequences are shown below each nucleotide sequence, with the predicted mature peptides underlined. Cysteine residues and stop codons, in the translated sequences are highlighted yellow and black, respectively














Gastridium	<i>C. (G.) geographus</i> 	GIIIA GIIIB GIIC	RD CC T-----O OKKCKDRQCK-OQRCCA* RD CC T-----O ORKCKDRRCK-OMKCCA* RD CC T-----O OKKCKDRRCK-OLKCCA*	
	<i>C. (G.) tulipa</i> 	TIIA	R HGCC K-----G OKGCS S RECR-OQHCC*	
Pionoconus	<i>C. (P.) striatus</i> 	SIIIA SIIIB	Z NCC N-----G GCS SK WCRDHARCC* Z NCC N-----G GCS SK WCKGHARCC*	
	<i>C. (P.) catus</i> 	CIIIA	G RCC E-----G PNGC SS RWCKDHARCC*	
	<i>C. (P.) stercusmuscarum</i> 	SmIIIA	Z RCC N-----G RRGC SS RWCRDHSRCC*	
	<i>C. (P.) magus</i> 	MIIIA	Z GCC N-----V PNGC SG RWCRDHAQCC*	
	<i>C. (P.) consors</i> 	CnIIIC CnIIIA CnIIIB	Z GCC N-----G PKGC SS KWCRDHARCC* G RCC D-----V PNAC SG RWCRDHAQCC* Z GCC G-----E PNLC F TRWC R NNARCCRQQ	
	<i>C. (P.) striolatus</i> 	SxIIIA SxIIIB SxIIIC	R CC T-----G KKGS CS GRACK-NLKCCA* Z KCC T-----G KKGS CS GRACK-NLRCCA* R GCC N-----G RGGCS -SR WCRDHARCC*	
Textilia	<i>C. (T.) bullatus</i> 	BuIIIA Bu3.5 BuIIIB BuIIIC Bu3.6 Bu3.7 BuIIIE Bu3.9 Bu3.10 Bu3.11 Bu3.12 BuIIID	V TDRCC K-----G KREC -SR WCRDHSRCC* VGDRCCK -----G KRGC -GR WCRDHSRCC* V GERCC K-----N GKRG C-GR WCRDHSRCC* I VDRCC N-----K GNGKRG C-SR WCRDHSRCC* IVDRCC N-----K GKGRRC -GR WCRDHSRCC* V GEHCCK -----K GNGKRG C-GR WCKGHARCC* V GEHCCRPRLRP --K PLWRGKREC -DR WCKSHSRCC* V GGNCCGPRRKP --K PYGQKGRAC -DR WCKSHSRCC* V GGNCCGPRRKP --K PYGRGKRAC -DR WCKSHSRCC* V GENCCRPKPTPKKKPKKNGKREC -DR WCKSHARCC* V GHTCCRPKPKPKKKPKQNGKAC -GR WCRDHARCC* V GLYCCRPKP -----N GQMMC -DR WCEKNSRCC*	
	<i>C. (T.) adamsonii</i> 	AdIIIA	R PVCC T-----G KGKRG CSS RWCRDHSRCC*	
	<i>C. (T.) dusaveli</i> 	DIIIA	R KVCC D-----G PNGC SS KWCKDHARCC*	
	Afonsoconus	<i>C. (A.) kinoshitai</i> 	KIIIA/B	N GCC N-----C SSKW CR DHSRCC*
		<i>C. (A.) bruuni</i> 	BIIIA	CC N-----K NGGC A GKWCKGRSRCC*

Fig. 3 Alignment of μ -conotoxin mature peptide sequences. Sequences reported in this study are in bold. Cysteine residues are highlighted yellow. Z, N-terminal pyroglutamate; O, hydroxyproline; *, C-terminal amidation

μ -Conotoxins BuIIIB, BuIIIE, DIIIA, AdIIIA and BIIIA have distinct selectivity profiles for human Na_v channel subtypes

We used automated whole-cell patch-clamp electrophysiology to determine the potency of each of the peptides at human Na_v 1.1–1.8.

The activity of BuIIIB has been investigated at rodent Na_v channels [18], but selectivity at human Na_v channels has not previously been reported. Here, BuIIIB was

most potent at hNa_v 1.3 ($IC_{50} = 5 \pm 1$ nM, $n = 4$ cells) and hNa_v 1.4 ($IC_{50} = 11 \pm 0.5$ nM, $n = 4$ cells), with ~5–10-fold selectivity over hNa_v 1.7 ($IC_{50} = 55 \pm 15$ nM, $n = 9$ cells), hNa_v 1.1 ($IC_{50} = 59 \pm 24$ nM, $n = 3$ cells) and hNa_v 1.2 ($IC_{50} = 79 \pm 13$ nM, $n = 5$ cells) and > 30-fold selectivity over hNa_v 1.6 ($IC_{50} = 171 \pm 53$ nM, $n = 4$ cells) (selectivity profile: $1.3 \approx 1.4 < 1.7 \approx 1.1 \approx 1.2 \approx 1.6$). BuIIIB was inactive at hNa_v 1.5 and hNa_v 1.8 when tested up to 10 μ M.

BuIIIE shared a similar selectivity profile ($1.3 \approx 1.4 < 1.1 \approx 1.2 \approx 1.6 \approx 1.7 < 1.5$) to BuIIIB but was less potent at

all subtypes tested. BuIIID, up to a concentration of 10 μM , had no effect on hNa_v1.4 or hNa_v1.7 current (Table 1), and was, therefore, not tested on other subtypes. A difference between BuIIID and all described μ -conotoxins, is the negatively charged residue (Glu) at position 21. In all μ -conotoxins described to date, this residue is a positively charged Arg or Lys. This charged residue has been identified as a key contributor to μ -conotoxin Na_v channel inhibition [13], and may explain the observed lack of inhibitory activity for BuIIID.

DIIIA was most potent at hNa_v1.3 ($\text{IC}_{50} = 185 \pm 3$ nM, $n = 3$ cells) and hNa_v1.4 ($\text{IC}_{50} = 216 \pm 45$ nM, $n = 4$ cells), and was also active at hNa_v1.1, hNa_v1.6 and hNa_v1.2 ($1.3 \approx 1.4 < 1.1 \approx 1.6 \approx 1.2$) but inactive (up to 10 μM) at hNa_v1.5, hNa_v1.7 and hNa_v1.8 (Fig. 4, Table 1). AdIIIA was most potent at hNa_v1.4 ($\text{IC}_{50} = 26 \pm 2$ nM, $n = 7$ cells) with a selectivity profile of ($1.4 < 1.1 \approx 1.7 \approx 1.3 < 1.2 < 1.6$) and was inactive (up to 10 μM) at hNa_v1.5 and hNa_v1.8 (Fig. 4, Table 1). BIIIA was most potent at hNa_v1.2 ($\text{IC}_{50} = 167 \pm 27$ nM, $n = 4$ cells) with ~ 3.5 -fold selectivity over hNa_v1.1 and hNa_v1.4 and a selectivity profile of ($1.2 < 1.1 \approx 1.4 < 1.7 \approx 1.3$). It was inactive (up to 10 μM) at hNa_v1.5, hNa_v1.6 and hNa_v1.8 (Fig. 4, Table 1).

The BIIIA[CysI–CysV, CysII–CysIV, CysIII–CysVI] isomer (BIIIA-iso2) had a similar activity profile to BIIIA, but with increased potency at hNa_v1.4 ($\text{IC}_{50} = 78 \pm 12$ nM, $n = 4$ cells) and decreased potency at hNa_v1.2 ($\text{IC}_{50} = 398 \pm 17$ nM, $n = 3$ cells) (Fig. 5, Table 1) and the selectivity profile $1.4 < 1.2 \approx 1.1 < 1.7 < 1.3$.

Discussion

Venoms are a promising source of novel peptides with potential utility as research tools and/or therapeutics [39]. RNA-seq of venom-producing tissues has become a common strategy for the identification of new venom peptides [40]. In this study, using RNA-seq we identified a total of 12 μ -conotoxin/ μ -conotoxin-like sequences from *C. (T.) bullatus*. This included three of the four previously reported

Fig. 4 μ -Conotoxins BuIIIB, BuIIIE, DIIIA, AdIIIA and BIIIA have distinct selectivity profiles for human Na_v channel subtypes. **a** Representative traces for human Na_v channel subtypes 1.1–1.8 in the presence of BuIIIB (100 nM). **b** Concentration–response curves for BuIIIB at human Na_v channel subtypes 1.1–1.8. **c** pIC_{50} for BuIIIB at human Na_v channel subtypes 1.1–1.8. **d–f** equivalent data for BuIIIE. **g–i** Equivalent data for DIIIA. **j–l** Equivalent data for AdIIIA. **m–o** Equivalent data for BIIIA. Data are mean \pm SEM

sequences (BuIIIA, BuIIIB and BuIIIC) [17] and a closely related homologue of Bu17 [32] (BuIIID). The additional sequences reported in this study, compared with the previous two studies, may reflect the greater depth of sequencing of our RNA-seq approach, although we cannot rule out other possibilities, such as intraspecific variation. Similarly, differences in sequencing technology may explain why 12 μ -conotoxin/ μ -conotoxin-like sequences were detected in *C. (T.) bullatus*, while only a single sequence was detected in each of the other species investigated using our Sanger sequencing approach. However, we cannot rule out other factors, including the possibility that these species have only one μ -conotoxin/ μ -conotoxin-like sequence, or that our approach was biased for the detection of individual sequences due to, e.g., differences in amplification rates. Future studies using different sequencing technology will be necessary to resolve these questions.

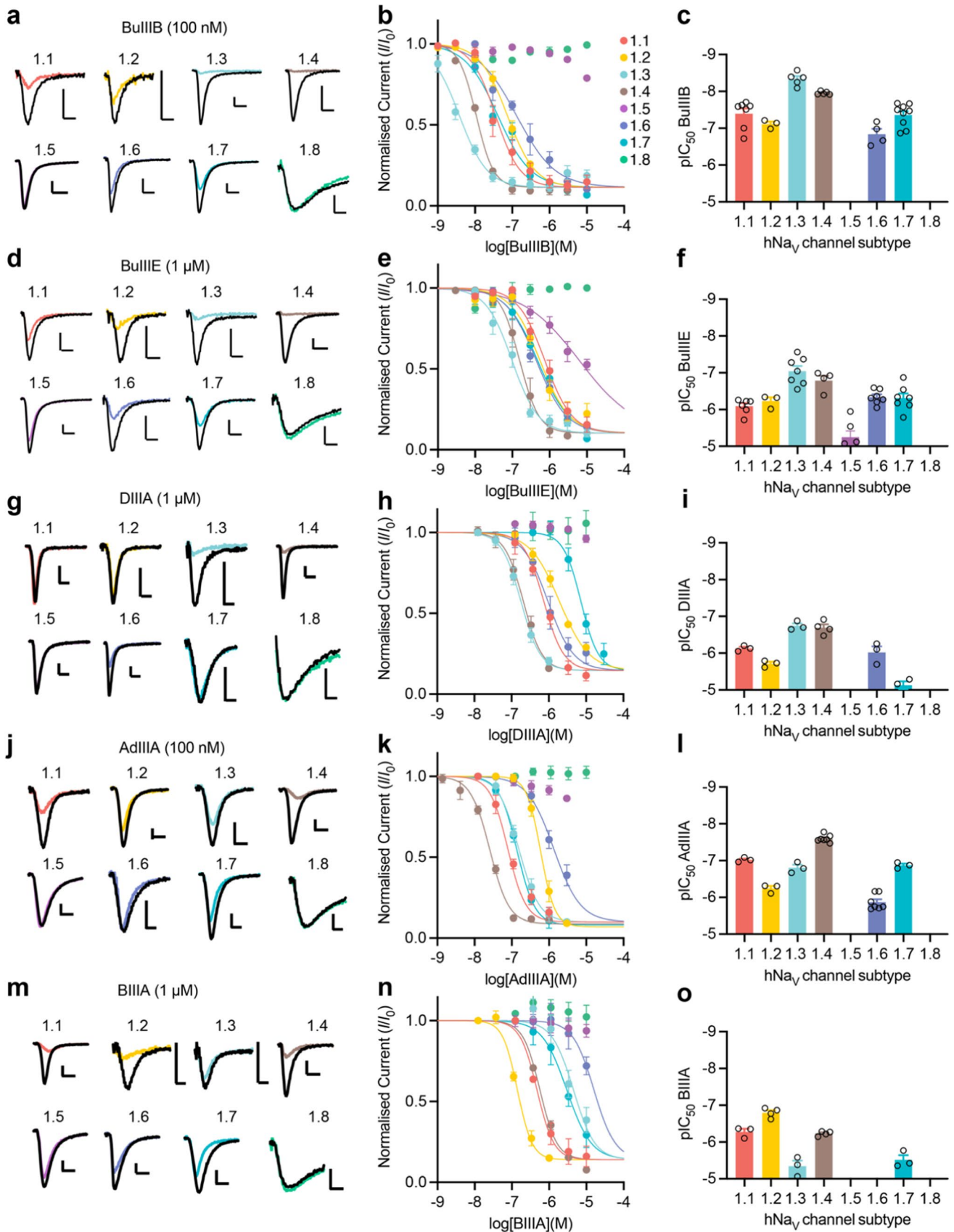
While high-output RNA-seq clearly has advantages over lower output methods for the identification of novel sequences, it still suffers from several limitations including a greater error rate compared with Sanger sequencing (which can lead to overestimation of sequence diversity [41]) and the poor performance of k-mer-based assembly algorithms in assembling multi-copy transcript families from short reads [42]. Indeed, with default settings, Trinity assembled only three of the 12 sequences correctly (BuIIIA, BuIIIC and Bu3.11). Only after remapping these sequences using the map-to-reference-tool of Geneious [30], did we identify and validate 12 sequences.

The most obvious limitation of an RNA-seq approach is the requirement for intact RNA—RNA rapidly degrades in non-living tissue, and RNA-seq approaches are, therefore,

Table 1 Potency (nM) of μ -conotoxins at human Na_v channel subtypes. Data are mean \pm SEM

nM	Na _v 1.1	Na _v 1.2	Na _v 1.3	Na _v 1.4	Na _v 1.5	Na _v 1.6	Na _v 1.7	Na _v 1.8
BuIIIB	59 \pm 24	79 \pm 13	5 \pm 1	11 \pm 0.5	> 10,000	171 \pm 53	55 \pm 15	> 10,000
BuIIID	n.d	n.d	n.d	> 10,000	n.d	n.d	> 10,000	n.d
BuIIIE	911 \pm 213	643 \pm 167	121 \pm 36	193 \pm 72	7555 \pm 2014	503 \pm 83	633 \pm 185	> 10,000
DIIIA	749 \pm 76	1971 \pm 238	185 \pm 27	216 \pm 45	> 10,000	1117 \pm 451	7900 \pm 1969	> 10,000
AdIIIA	96 \pm 8	587 \pm 97	163 \pm 30	26 \pm 2	> 10,000	1479 \pm 223	137 \pm 15	> 10,000
BIIIA	557 \pm 116	167 \pm 27	5172 \pm 1828	595 \pm 45	> 10,000	> 10,000	3304 \pm 823	> 10,000
BIIIA-iso2	568 \pm 179	398 \pm 17	8316 \pm 1205	78 \pm 12	> 10,000	> 10,000	2486 \pm 572	> 10,000

n.d., not determined



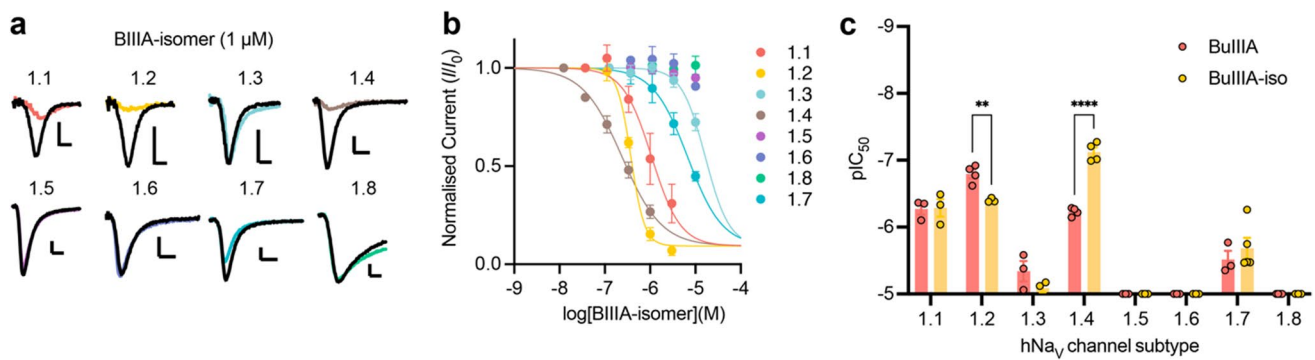


Fig. 5 [CysI–CysV, CysII–CysIV, CysIII–CysVI] isomer (BIIIA-iso2) of μ -conotoxin BIIIA has subtle changes in its selectivity profile for human Na_V channel subtypes. **a** Representative traces for human Na_V channel subtypes 1.1–1.8 in the presence of BIIIA-iso2

(1 μM). **b** Concentration–response curves for BIIIA-isomer at human Na_V channel subtypes 1.1–1.8. **c** Comparison of pIC_{50} for BIIIA and BIIIA-iso2 at human Na_V channel subtypes 1.1–1.8. Data are mean SEM. ** $P < 0.01$; **** $P < 0.0001$; unpaired t test

not possible in the absence of fresh tissue. While we could not obtain fresh or adequately preserved venom gland tissues for species of the subgenera *Afonsoconus* or *Textilia* other than *C. (T.) bullatus*, we were able to obtain tissue samples from historical specimens. DNA is more stable than RNA and from these specimens we were able to extract intact DNA and from this, identify μ -conotoxins. The study of DNA from historical museum specimens has found a number of applications in biology [43]. In this study we were “bioprospecting” for molecules with potential utility in physiology and medicine. As shown here, this approach is useful for identifying specific sequences of interest from samples that are otherwise unavailable, e.g., rare, endangered or extinct organisms. However, it is subject to some limitations: the specimen must be available in a collection and while we did not explicitly test this here, there are limitations associated with the age and storage conditions of specimens. Here, we were targeting a relatively short stretch of sequence ~ 1500 b, from samples that had been stored in ethanol (various concentrations) for a maximum of 11 y. Increased DNA fragmentation would be expected for older or poorly stored samples.

This approach is not suitable for the de novo identification of protein sequences. Prior knowledge of homologous sequences was critical in enabling the design of primers and prediction of mature peptide sequences and post-translational modifications (PTMs) (e.g., C-terminal amidation) including prediction of cystine connectivity. In this study sufficient information from homologous sequences facilitated our prediction of the N- and C-termini of the mature peptides. Similarly, on the basis of previous studies it was facile to predict amidation of the peptide C-termini. Several μ -conotoxins have one or more proline to hydroxyproline post-translation modifications [6, 36, 44]; each of the μ -conotoxins in this study, except BIIIA, have one or more proline residues in their sequence and it is

possible that the native form of the toxins in the respective venoms also have these modifications; however, we were unable to make any confident predictions in this respect, and each conotoxin was synthesized without this PTM. Another important PTM is disulfide bond formation. Of the native μ -conotoxins for which disulfide connectivity has been investigated all have a cystine connectivity of CysI–CysIV, CysII–CysV, CysIII–CysVI [34, 35], as do active synthetic μ -conotoxins [36, 37]. On the basis of these studies, we synthesized our μ -conotoxins with this “canonical” cystine connectivity. However, it remains possible that the native forms in the venom may have a different cystine connectivity. For example, KIIIA, which under certain in vitro folding conditions favours a CysI–CysV, CysII–CysIV, CysIII–CysVI connectivity is more potent at $\text{rNa}_V1.2$ and $\text{hNa}_V1.2$ than the peptide with the canonical cystine connectivity [38, 45]. In this study, we synthesized two isomers of BIIIA, one with the canonical cystine connectivity and one with the alternative CysI–CysV, CysII–CysIV, CysIII–CysVI connectivity. Both isomers were active, the major difference being reduced potency at $\text{hNa}_V1.2$ and increased potency at $\text{hNa}_V1.4$ for the isomer with the alternative connectivity. These data provide more evidence that at least some μ -conotoxins can tolerate the aforementioned change in cystine connectivity with relatively subtle, but potentially important changes to their selectivity profiles.

The selectivity profile of BuIIIB at human Na_V channels is distinct from that reported in previous studies. Previous studies using rodent Na_V channels reported a selectivity profile of $1.4 < 1.2 < 1.3 < 1.1 < 1.6 < 1.5$ with potencies (K_d) of 3.6 and 200 nM for $\text{rNa}_V1.4$ and $\text{rNa}_V1.3$, respectively [18]. Here, in human Na_V overexpression systems, we observed a selectivity profile for BuIIIB of $1.3 \approx 1.4 < 1.7 \approx 1.1 \approx 1.2 \approx 1.6$, with potencies of 5 and 11 nM for $\text{rNa}_V1.4$ and $\text{rNa}_V1.3$, respectively. Some of the earliest studies of μ -conotoxins

reported differences between channels of different species. For example, KIIIA blocked TTX-resistant Na^+ currents in frog (*Rana pipiens*) neuronal preparations, but had limited effects on action potentials in skeletal muscle (TTX-sensitive) [11]. In a subsequent study, using rat channels, KIIIA did not inhibit TTX-resistant subtypes, but potently inhibited TTX-sensitive subtypes with a selectivity profile of $1.2 < 1.4 < 1.7 \approx 1.1 < 1.3$ [46]. Similar differences have been observed with other μ -conotoxins [47]. Furthermore, KIIIA has a distinct selectivity profile for human Na_v channels ($1.4 < 1.1 < 1.2 < 1.7 < 1.6 < 1.3$) [48]. It is possible that these differences arise from the use of different techniques (e.g., two-electrode voltage- or patch-clamp methods on oocytes vs. mammalian cells) or different Na_v channel auxiliary subunit composition [49]; however, the most congruent explanation is that there are differences in the structure of the μ -conotoxin binding site between homologous channels of different species.

While there are differences in subtype selectivity profiles, all of the μ -conotoxins described so far, including those presented in this study, invariably share potent activity at $\text{Na}_v1.4$. When viewed from a drug discovery perspective, activity at $\text{Na}_v1.4$ is typically considered undesirable and most efforts to engineer μ -conotoxins have focused on increasing selectivity for potential therapeutic targets, e.g., $\text{Na}_v1.7$ or $\text{Na}_v1.3$ over $\text{Na}_v1.4$ [10]. However, it is important to consider that in some systems, e.g., the peripheral and central nervous systems, $\text{Na}_v1.4$ is absent. When this is taken into consideration, certain μ -conotoxins may find utility as research tools in delineating the physiological roles of specific Na_v channel subtypes in certain isolated systems. For example, BuIIIB, with an IC_{50} of 5 ± 1 nM at $\text{hNa}_v1.3$, is \sim tenfold selective over other neuronal hNa_v subtypes. BuIIIB has the potential to serve as a tool for investigating the role of $\text{Na}_v1.3$ in the human nervous system, and as a template for engineering more selective $\text{hNa}_v1.3$ blockers.

Together, this study contributes new information on μ -conotoxin structure–activity relationship (SAR): BuIID informs on the sequence features that drive activity at Na_v channels in general; BuIIIB, BuIIIE and DIIIA may inform on the sequence features that drive potency at $\text{hNa}_v1.3$ over other neuronal subtypes; Similarly, BIIIA and AdIIIA may inform on the sequence features that drive potency at $\text{hNa}_v1.2$ and $\text{hNa}_v1.4$, respectively, over other Na_v subtypes; Finally, among the seven μ -conotoxins tested in this study, three (BuIIB, BuIIIE and AdIIIA) were potent blockers of $\text{hNa}_v1.7$. While not selective for $\text{hNa}_v1.7$, these μ -conotoxins could potentially offer new insight into the sequence features driving potency at this subtype.

Supplementary Information The online version contains supplementary material available at <https://doi.org/10.1007/s00018-023-04935-0>.

Acknowledgements We thank: Noel Saguil for collection of *C. (T.) bullatus*; Nicolas Puillandre and Philippe Bouchet (MNHN) for providing the tissue samples of *C. (A.) brunni* and *C. (T.) adamsonii*; Samuel Espino for the photograph of the shell of *C. (T.) dusaveli*.

Author contributions Conceptualisation, SDR; methodology, IV and SDR; investigation, KLM, HO, CIS, JRD, DV, DH, BG, QL, PKB, HS and SDR; writing—original draft, SDR; writing—review and editing, all authors; funding acquisition, IV, BMO and SDR; resources, MY, BMO, IV and SDR; supervision, MY, IV, BMO and SDR.

Funding Open Access funding enabled and organized by CAUL and its Member Institutions. I.V. and S.D.R. are supported by Australian National Health and Medical Research Council Investigator grants (2017086 and 2017461). J.D. is supported by an Australian Research Council Discovery Early Career Research Award (DE210100422).

Availability of data and materials The nucleotide sequences of Bu3.4 (BuIID), Bu3.8 (BuIIIE), Bu3.5, Bu3.6, Bu3.7, Bu3.9, Bu3.10, Bu3.11, Bu3.12, D3.1, Ad3.1 (including its intronic sequence) and B3.1 have been deposited at DDBJ/EMBL/GenBank [Accessions: OR128446-OR128457]. Sequences of all additional conotoxins identified in the venom gland transcriptome of *C. (T.) bullatus* are provided as Supplementary file 2.

Code availability Not applicable.

Declarations

Conflict of interest C.I. Schroeder is an employee of Genentech Inc. and a shareholder of Roche.

Ethics approval Not applicable.

Consent to participate Not applicable.

Consent for publication Not applicable.

Open Access This article is licensed under a Creative Commons Attribution 4.0 International License, which permits use, sharing, adaptation, distribution and reproduction in any medium or format, as long as you give appropriate credit to the original author(s) and the source, provide a link to the Creative Commons licence, and indicate if changes were made. The images or other third party material in this article are included in the article's Creative Commons licence, unless indicated otherwise in a credit line to the material. If material is not included in the article's Creative Commons licence and your intended use is not permitted by statutory regulation or exceeds the permitted use, you will need to obtain permission directly from the copyright holder. To view a copy of this licence, visit <http://creativecommons.org/licenses/by/4.0/>.

References

1. Catterall WA, Goldin AL, Waxman SG (2005) International Union of Pharmacology. XLVII. Nomenclature and structure–function relationships of voltage-gated sodium channels. *Pharmacol Rev* 57(4):397–409
2. Mantegazza M, Curia G, Biagini G, Ragsdale DS, Avoli M (2010) Voltage-gated sodium channels as therapeutic targets in epilepsy and other neurological disorders. *Lancet Neurol* 9(4):413–424
3. Catterall WA, Cestele S, Yarov-Yarovoy V, Yu FH, Konoki K, Scheuer T (2007) Voltage-gated ion channels and gating modifier toxins. *Toxicol* 49(2):124–141

4. Stevens M, Peigneur S, Tytgat J (2011) Neurotoxins and their binding areas on voltage-gated sodium channels. *Front Pharmacol* 2:71
5. Deuis JR, Mueller A, Israel MR, Vetter I (2017) The pharmacology of voltage-gated sodium channel activators. *Neuropharmacology* 127:87–108
6. Cruz LJ, Gray WR, Olivera BM, Zeikus RD, Kerr L, Yoshikami D, Moczydlowski E (1985) *Conus geographus* toxins that discriminate between neuronal and muscle sodium channels. *J Biol Chem* 260(16):9280–9288
7. Yanagawa Y, Abe T, Satake M (1987) μ -Conotoxins share a common binding site with tetrodotoxin/saxitoxin on eel electroplax Na channels. *J Neurosci* 7(5):1498–1502
8. Corpuz GP, Jacobsen RB, Jimenez EC, Watkins M, Walker C, Colledge C, Garrett JE, McDougal O, Li W, Gray WR, Hillyard DR, Rivier J, McIntosh JM, Cruz LJ, Olivera BM (2005) Definition of the M-conotoxin superfamily: characterization of novel peptides from molluscivorous *Conus venoms*. *Biochemistry* 44(22):8176–8186
9. Robinson SD, Norton RS (2014) Conotoxin gene superfamilies. *Mar Drugs* 12(12):6058–6101
10. Green BR, Bulaj G, Norton RS (2014) Structure and function of μ -conotoxins, peptide-based sodium channel blockers with analgesic activity. *Future Med Chem* 6(15):1677–1698
11. Bulaj G, West PJ, Garrett JE, Watkins M, Zhang MM, Norton RS, Smith BJ, Yoshikami D, Olivera BM (2005) Novel conotoxins from *Conus striatus* and *Conus kinoshitai* selectively block TTX-resistant sodium channels. *Biochemistry* 44(19):7259–7265
12. Khoo KK, Feng ZP, Smith BJ, Zhang MM, Yoshikami D, Olivera BM, Bulaj G, Norton RS (2009) Structure of the analgesic μ -conotoxin KIIIA and effects on the structure and function of disulfide deletion. *Biochemistry* 48(6):1210–1219
13. McArthur JR, Singh X, McMaster D, Winkfein R, Tieleman DP, French RJ (2011) Interactions of key charged residues contributing to selective block of neuronal sodium channels by μ -conotoxin KIIIA. *Mol Pharmacol* 80(4):573–584
14. Han TS, Zhang MM, Walewska A, Gruszczynski P, Robertson CR, Cheatham TE 3rd, Yoshikami D, Olivera BM, Bulaj G (2009) Structurally minimized μ -conotoxin analogues as sodium channel blockers: implications for designing conopeptide-based therapeutics. *Chemmedchem* 4(3):406–414
15. Van Der Haegen A, Peigneur S, Tytgat J (2011) Importance of position 8 in μ -conotoxin KIIIA for voltage-gated sodium channel selectivity. *FEBS J* 278(18):3408–3418
16. Pan X, Li Z, Huang X, Huang G, Gao S, Shen H, Liu L, Lei J, Yan N (2019) Molecular basis for pore blockade of human Na⁺ channel NaV1.2 by the μ -conotoxin KIIIA. *Science* 363(6433):1309–1313
17. Holford M, Zhang MM, Gowd KH, Azam L, Green BR, Watkins M, Ownby JP, Yoshikami D, Bulaj G, Olivera BM (2009) Pruning nature: biodiversity-derived discovery of novel sodium channel blocking conotoxins from *Conus bullatus*. *Toxicon* 53(1):90–98
18. Wilson MJ, Yoshikami D, Azam L, Gajewiak J, Olivera BM, Bulaj G, Zhang MM (2011) μ -Conotoxins that differentially block sodium channels Na_v1.1 through 18 identify those responsible for action potentials in sciatic nerve. *Proc Natl Acad Sci USA* 108(25):10302–10307
19. Kuang Z, Zhang MM, Gupta K, Gajewiak J, Gulyas J, Balaran P, Rivier JE, Olivera BM, Yoshikami D, Bulaj G, Norton RS (2013) Mammalian neuronal sodium channel blocker *mu*-conotoxin BuIIIB has a structured N-terminus that influences potency. *ACS Chem Biol* 8(6):1344–1351
20. Green BR, Zhang MM, Chhabra S, Robinson SD, Wilson MJ, Redding A, Olivera BM, Yoshikami D, Bulaj G, Norton RS (2014) Interactions of disulfide-deficient selenocysteine analogs of μ -conotoxin BuIIIB with the α -subunit of the voltage-gated sodium channel subtype 1.3. *FEBS J* 281(13):2885–2898
21. Dance SP (1969) Rare shells. Faber and Faber Limited, London
22. Powell AWB (1958) Mollusca of the Kermadec Islands: part I. *Rec Auckland Inst Museum* 5(1/2):65–85
23. Puillandre N, Duda TF, Meyer C, Olivera BM, Bouchet P (2015) One, four or 100 genera? A new classification of the cone snails. *J Molluscan Stud* 81(1):1–23
24. Pertea G (2015) fqtrim: v0.9.4 release. <https://doi.org/10.5281/zenodo.20552>
25. Schmieder R, Edwards R (2011) Quality control and preprocessing of metagenomic datasets. *Bioinformatics* 27(6):863–864
26. Haas BJ, Papanicolaou A, Yassour M, Grabherr M, Blood PD, Bowden J, Couger MB, Eccles D, Li B, Lieber M, MacManes MD, Ott M, Orvis J, Pochet N, Strozzi F, Weeks N, Westerman R, William T, Dewey CN, Henschel R, LeDuc RD, Friedman N, Regev A (2013) De novo transcript sequence reconstruction from RNA-seq using the Trinity platform for reference generation and analysis. *Nat Protocol* 8(8):1494–1512
27. Altschul SF, Gish W, Miller W, Myers EW, Lipman DJ (1990) Basic local alignment search tool. *J Mol Biol* 215(3):403–410
28. Kaas Q, Westermann JC, Craik DJ (2010) Conopeptide characterization and classifications: an analysis using ConoServer. *Toxicon* 55(8):1491–1509
29. Li B, Dewey CN (2011) RSEM: accurate transcript quantification from RNA-Seq data with or without a reference genome. *BMC Bioinform* 12(1):323
30. Kears M, Moir R, Wilson A, Stones-Havas S, Cheung M, Sturrock S, Buxton S, Cooper A, Markowitz S, Duran C, Thierer T, Ashton B, Meintjes P, Drummond A (2012) Geneious basic: an integrated and extendable desktop software platform for the organization and analysis of sequence data. *Bioinformatics* 28(12):1647–1649
31. Vetter I, Lewis RJ (2010) Characterization of endogenous calcium responses in neuronal cell lines. *Biochem Pharmacol* 79(6):908–920
32. Hu H, Bandyopadhyay PK, Olivera BM, Yandell M (2011) Characterization of the *Conus bullatus* genome and its venom-duct transcriptome. *BMC Genomics* 12(1):60
33. Wu Y, Wang L, Zhou M, You Y, Zhu X, Qiang Y, Qin M, Luo S, Ren Z, Xu A (2013) Molecular evolution and diversity of *Conus* peptide toxins, as revealed by gene structure and intron sequence analyses. *PLoS ONE* 8(12):e82495
34. Hidaka Y, Sato K, Nakamura H, Kobayashi J, Ohizumi Y, Shimonishi Y (1990) Disulfide pairings in geographotoxin I, a peptide neurotoxin from *Conus geographus*. *FEBS Lett* 264(1):29–32
35. Schroeder CI, Ekberg J, Nielsen KJ, Adams D, Loughnan ML, Thomas L, Adams DJ, Alewood PF, Lewis RJ (2008) Neuronally selective μ -conotoxins from *Conus striatus* utilize an α -helical motif to target mammalian sodium channels. *J Biol Chem* 283(31):21621–21628
36. Shon K-J, Olivera BM, Watkins M, Jacobsen RB, Gray WR, Floresca CZ, Cruz LJ, Hillyard DR, Brink A, Terlau H, Yoshikami D (1998) μ -Conotoxin PIIIA, a new peptide for discriminating among tetrodotoxin-sensitive Na channel subtypes. *J Neurosci* 18(12):4473
37. Keizer DW, West PJ, Lee EF, Yoshikami D, Olivera BM, Bulaj G, Norton RS (2003) Structural basis for tetrodotoxin-resistant sodium channel binding by μ -conotoxin SmIIIA. *J Biol Chem* 278(47):46805–46813
38. Khoo KK, Gupta K, Green BR, Zhang MM, Watkins M, Olivera BM, Balaran P, Yoshikami D, Bulaj G, Norton RS (2012) Distinct disulfide isomers of *mu*-conotoxins KIIIA and KIIIB block voltage-gated sodium channels. *Biochemistry* 51(49):9826–9835
39. King GF (2011) Venoms as a platform for human drugs: translating toxins into therapeutics. *Expert Opin Biol Ther* 11(11):1469–1484

40. Robinson SD, Undheim EAB, Ueberheide B, King GF (2017) Venom peptides as therapeutics: advances, challenges and the future of venom-peptide discovery. *Expert Rev Proteomics* 14(10):931–939
41. Lavergne V, Harliwong I, Jones A, Miller D, Taft RJ, Alewood PF (2015) Optimized deep-targeted proteotranscriptomic profiling reveals unexplored *Conus* toxin diversity and novel cysteine frameworks. *Proc Natl Acad Sci USA* 112(29):E3782–3791
42. Macrander J, Broe M, Daly M (2015) Multi-copy venom genes hidden in de novo transcriptome assemblies, a cautionary tale with the snakelocks sea anemone *Anemonia sulcata* (Pennant, 1977). *Toxicon* 108:184–188
43. Raxworthy CJ, Smith BT (2021) Mining museums for historical DNA: advances and challenges in museomics. *Trends Ecol Evol* 36(11):1049–1060
44. Lewis RJ, Schroeder CI, Ekberg J, Nielsen KJ, Loughnan M, Thomas L, Adams DA, Drinkwater R, Adams DJ, Alewood PF (2007) Isolation and structure-activity of μ -conotoxin TIIIA, a potent inhibitor of tetrodotoxin-sensitive voltage-gated sodium channels. *Mol Pharmacol* 71(3):676–685
45. Tran HNT, McMahon KL, Deuis JR, Vetter I, Schroeder CI (2022) Structural and functional insights into the inhibition of human voltage-gated sodium channels by μ -conotoxin KIIIA disulfide isomers. *J Biol Chem* 298(3):101728
46. Zhang MM, Green BR, Catlin P, Fiedler B, Azam L, Chadwick A, Terlau H, McArthur JR, French RJ, Gulyas J, Rivier JE, Smith BJ, Norton RS, Olivera BM, Yoshikami D, Bulaj G (2007) Structure/function characterization of μ -conotoxin KIIIA, an analgesic, nearly irreversible blocker of mammalian neuronal sodium channels. *J Biol Chem* 282(42):30699–30706
47. Zhang MM, Fiedler B, Green BR, Catlin P, Watkins M, Garrett JE, Smith BJ, Yoshikami D, Olivera BM, Bulaj G (2006) Structural and functional diversities among μ -conotoxins targeting TTX-resistant sodium channels. *Biochemistry* 45(11):3723–3732
48. McMahon KL, Tran HNT, Deuis JR, Craik DJ, Vetter I, Schroeder CI (2022) μ -conotoxins targeting the human voltage-gated sodium channel subtype $\text{Na}_v1.7$. *Toxins* 14(9):600
49. Zhang MM, Wilson MJ, Azam L, Gajewiak J, Rivier JE, Bulaj G, Olivera BM, Yoshikami D (2013) Co-expression of $\text{Na}_v\beta$ subunits alters the kinetics of inhibition of voltage-gated sodium channels by pore-blocking μ -conotoxins. *Br J Pharmacol* 168(7):1597–1610

Publisher's Note Springer Nature remains neutral with regard to jurisdictional claims in published maps and institutional affiliations.